Article

Hydrophobic Surfactant Proteins Strongly Induce Negative Curvature

Mariya Chavarha,[1,2,3] Ryan W. Loney,[1,2,3] Shankar B. Rananavare,[4] and Stephen B. Hall[1,2,3,*]
[1]Department of Biochemistry & Molecular Biology, [2]Department of Medicine, and [3]Department of Physiology & Pharmacology, Oregon Health & Science University, Portland, Oregon; and [4]Department of Chemistry, Portland State University, Portland, Oregon

ABSTRACT The hydrophobic surfactant proteins SP-B and SP-C greatly accelerate the adsorption of vesicles containing the surfactant lipids to form a film that lowers the surface tension of the air/water interface in the lungs. Pulmonary surfactant enters the interface by a process analogous to the fusion of two vesicles. As with fusion, several factors affect adsorption according to how they alter the curvature of lipid leaflets, suggesting that adsorption proceeds via a rate-limiting structure with negative curvature, in which the hydrophilic face of the phospholipid leaflets is concave. In the studies reported here, we tested whether the surfactant proteins might promote adsorption by inducing lipids to adopt a more negative curvature, closer to the configuration of the hypothetical intermediate. Our experiments used x-ray diffraction to determine how the proteins in their physiological ratio affect the radius of cylindrical monolayers in the negatively curved, inverse hexagonal phase. With binary mixtures of dioleoylphosphatidylethanolamine (DOPE) and dioleoylphosphatidylcholine (DOPC), the proteins produced a dose-related effect on curvature that depended on the phospholipid composition. With DOPE alone, the proteins produced no change. With an increasing mol fraction of DOPC, the response to the proteins increased, reaching a maximum 50% reduction in cylindrical radius at 5% (w/w) protein. This change represented a doubling of curvature at the outer cylindrical surface. The change in spontaneous curvature, defined at approximately the level of the glycerol group, would be greater. Analysis of the results in terms of a Langmuir model for binding to a surface suggests that the effect of the lipids is consistent with a change in the maximum binding capacity. Our findings show that surfactant proteins can promote negative curvature, and support the possibility that they facilitate adsorption by that mechanism.

INTRODUCTION

Fusogenic peptides may provide a particularly simple example of proteins that affect the curvature of lipids (1). These short amino acid sequences promote the fusion of two bilayers. The initial merger between the two outer leaflets of the fusing bilayers supports a process that begins with the formation of a stalk connecting the two membranes (2). The leaflets composing the stalk would bend back upon themselves to achieve the correct orientation at each bilayer. The leaflets would have negative curvature, defined by the concave shape of their hydrophilic surfaces. Several compounds alter rates of fusion according to how they affect spontaneous curvature (3), which monolayers adopt in the absence of applied force (4). A spontaneous curvature closer to the configuration of the stalk would reduce the energy of bending required to form the proposed intermediate. Induction of negative curvature would provide a simple explanation for how the fusogenic peptides achieve their function.

Direct evidence, however, that these peptides can make the proposed changes in curvature has been limited (5). There is a growing list of proteins that can produce positive curvature, either by binding to a leaflet and imposing their intrinsic shape or by inserting superficially into the face of a leaflet and preferentially expanding the hydrophilic regions (1,6). Induction of negative curvature would instead require a greater expansion of the hydrophobic side of the monolayer. Measurements with the unpaired monolayers of the inverse hexagonal (H_{II}) phase (Fig. 1 *A*) can detect how added constituents affect spontaneous curvature. Diffraction from the cylindrical monolayers has provided a few examples of fusogenic peptides that enhance negative curvature (7–12), but the changes have been small.

The studies reported here address the effect on curvature of the hydrophobic surfactant proteins SP-B and SP-C. These proteins promote the fusion of vesicles in vitro (13,14) and fit within the class of fusogenic peptides. The proteins also greatly accelerate adsorption of the surfactant lipids to form the thin film that lowers the surface tension of the alveolar air/water interface (15). This activity may well represent their physiological function. Adsorption of the surfactant vesicles occurs by a process analogous to fusion. The components of surfactant vesicles insert into the interface collectively (16–18). As with fusion, several compounds affect adsorption according to how they alter curvature (19–23). These results suggest that surfactant proteins might accelerate adsorption by facilitating the formation of a negatively curved, rate-limiting intermediate (Fig. 1 *B*) analogous to the stalk proposed for fusion (24–26). Direct measurements with H_{II} structures have shown that the surfactant proteins can promote more negative curvature, but their effect is limited, amounting to a change of only ~8% (22).

Submitted November 26, 2014, and accepted for publication May 28, 2015.

*Correspondence: sbh@ohsu.edu

Editor: David Cafiso.

0006-3495/15/07/0095/11 $2.00

http://dx.doi.org/10.1016/j.bpj.2015.05.030

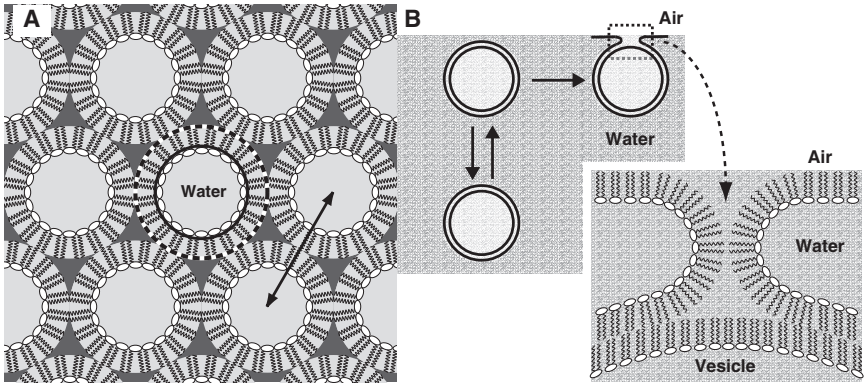

FIGURE 1 Diagrams of pertinent curved structures. (*A*) Structure of the H_{II} phase. The double-headed arrow indicates the lattice constant measured by diffraction. The solid circle approximates the location of the pivotal plane, at which the spontaneous curvature is estimated. The dashed circle gives the location of the outer surface of the cylindrical monolayer, the radius of which determines c^{out}. (*B*) Hypothetical rate-limiting intermediate involved in the adsorption of phospholipid vesicles to an air/water interface (25).

The ability of the surfactant proteins to change the curvature of lipids is not universal. In the H_{II} phase formed by dioleoylphosphatidylethanolamine (DOPE), the proteins have no effect (22). The change in curvature produced by the proteins occurs with dioleoylphosphatidylglycerol (DOPG) added to DOPE (DOPE:DOPG, 9:1 mol/mol) to replicate the ~10% content of anionic lipids in pulmonary surfactant (27). The effect of DOPG could reflect electrostatic interactions between the cationic proteins and the anionic lipid. SP-B and SP-C have a net charge of +14 (28) and +2–3 (29), respectively. Salt, however, which should screen electrostatic effects, produces a remarkably limited change (22).

In addition to introducing negative charge, DOPG also expands the H_{II} cylinders (22,30). This observation suggests that DOPG might alter the effect of the proteins by changing the dimensions of the cylindrical monolayers rather than by affecting the charge. In lamellar bilayers, the spontaneous curvature of lipids can affect binding to other hydrophobic peptides (31). Zwitterionic dioleoylphosphatidylcholine (DOPC) expands the H_{II} phase formed by DOPE (32) without affecting charge. Here, we used DOPC to test whether the measured effect of the proteins on curvature depends on the radius of the H_{II} cylinders.

MATERIALS AND METHODS

DOPC (Avanti Polar Lipids, Alabaster, AL), DOPE (Avanti Polar Lipids), and tetradecane (n-tetradecane; MP Biomedicals, Solon, OH) were used without further characterization or purification. Extracted calf surfactant, obtained from Dr. Edmund Egan (ONY, Amherst, NY), provided the source of the hydrophobic surfactant proteins, which were separated in their physiological ratio from the surfactant lipids by gel permeation chromatography (33–35). SP-B and SP-C isolated by this procedure have the expected characteristics (36,37). SP-B migrates electrophoretically on gels as a reducible homodimer of monomers containing 79 amino acids. SP-C has the appropriate mobility for a monomer of 35 amino acids. Calculations on the molar content of the proteins assumed equal weights for SP-B and SP-C (38), and molecular weights of 17,397 Da for SP-B and 4,042 Da for SP-C (39).

The constituents of the experimental samples were combined in chloroform, which was removed initially under a stream of nitrogen, followed by incubation overnight at an ambient pressure of 2 mbar. After hydration overnight in buffered electrolyte (HSC: 10 mM Hepes pH 7.0, 150 mM NaCl, 1.5 mM $CaCl_2$) at a phospholipid concentration of 50 mM, the samples were resuspended by repeated freezing and thawing, followed by vigorous vortexing. The samples were transferred to capillaries, which were then sealed. For measurements of small-angle x-ray scattering, the capillaries were mounted on a temperature-regulated aluminum block and heated to sequentially higher temperatures. Samples were equilibrated at each temperature for at least 10 min, which we established both here and in prior studies (22) as sufficient to achieve a signal that remained constant for hours. The samples were then exposed for 2 min to synchrotron radiation of wavelength 1.488 Å on beamline 1-4 at the Stanford Synchrotron Radiation Lightsource. The angular dependence of distance on the detector was calibrated with samples of silver behenate. Structural phases in the experimental samples were determined by fitting measured values of the momentum transfer, q, to $s = \sqrt{h^2 + hk + k^2}$ for hexagonal phases, and to $s = \sqrt{h^2 + k^2 + l^2}$ for other space groups, for allowed values of the Miller indices, h, k, *and* l (37,40). For the hexagonal phase, the slope of these plots provided the lattice constant, a_0, according to $a_0 = 4\,\pi/(\sqrt{3}\ slope)$. The curvature, c^{out}, at the outer surface of the cylindrical monolayers was calculated from $c^{out} = 2/a_0$.

A modified Langmuir equation,

$$c^{out} = \left\langle c_0^{out} \right\rangle + \frac{a_1\, SP}{1 + a_2\, SP}\, X_{PC},$$

expressed the variation of c^{out} with the total concentration of surfactant protein, *SP*, and the mol fraction of DOPC, X_{PC}, relative to $\langle c_0^{out} \rangle$, the averaged curvature for the lipids alone. The best fit of data to the equation minimized the square of the vertical error using the Levenberg-Marquardt algorithm implemented by the program Igor Pro (WaveMetrics, Lake Oswego, OR). This analysis omitted data at $X_{PC} = 0.9$ because of their wide scatter.

RESULTS

Mixtures with mol fractions of DOPC (X_{PC}) from 0.0 to 0.9 formed the H_{II} phase. These structures were identified by the powder diffraction obtained from dispersed samples exposed to synchrotron radiation. The characteristic spacing of at least three reflections (Fig. 2) established the presence of structures with the hexagonal p6m space group. Tetradecane, added at 16% (w/w) to minimize the unfavorable disruption of chain packing in curved phases (41), in most cases stabilized the H_{II} phase relative to lamellar or bicontinuous inverse cubic (Q_{II}) structures. Our analysis omitted samples that diffracted poorly or that produced diffraction from coexisting phases because of the uncertain composition of each structure.

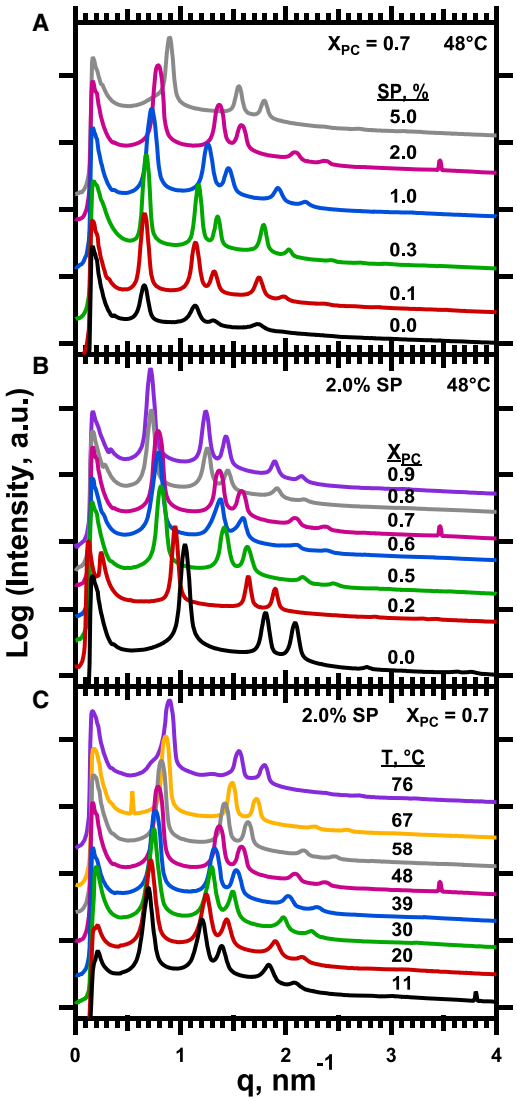

FIGURE 2 Diffraction from samples of DOPE:DOPC with 16% (w/w) tetradecane and the hydrophobic surfactant proteins. The traces give the radially integrated, diffracted intensity produced by the dispersed samples as a function of the momentum transfer, q. The traces are shifted vertically by arbitrary amounts without a change in scale for clarity of presentation. The different panels illustrate the effects of (*A*) the content of surfactant protein, (*B*) the composition of the phospholipids, and (*C*) temperature. To see this figure in color, go online.

The H_{II} lattice constant, which equals the diameter of the outer cylindrical surface (Fig. 1 *A*), provided access to the curvature, defined as the reciprocal of the radius (42), at the outer surface (c^{out}). We reported all values of curvature as their magnitudes, ignoring their uniformly negative sign. With each set of lipids, increasing concentrations of the surfactant proteins (*SP*) in their physiological ratio determined how they affected c^{out} (Fig. 3). Measurements were obtained after heating to different temperatures between 11°C and 90°C to provide an additional variable that altered the size of the cylinders (Fig. 3).

Lipids alone

Analysis of our results required a description of how the surfactant proteins, the composition of lipids, and temperature each affected c^{out}, and how the different variables altered the response to the other factors. We first considered the effect of the lipids without the proteins, which is well understood from prior studies (32,41), and then determined how the proteins modified that behavior.

c_0^{out}, the outer curvature for lipids without proteins, changed linearly with X_{PC} (Fig. 4). For c_{PC}^{out} and c_{PE}^{out}, the outer curvatures for samples containing only DOPC or DOPE, respectively, and the difference between them, $\Delta = c_{PC}^{out} - c_{PE}^{out}$, the outer curvature followed the relationship $c_0^{out} = c_{PE}^{out} + \Delta X_{PC}$. The linear fits of c_0^{out} versus X_{PC} at each temperature provided average values for the curvature of the lipids alone, $<c_0^{out}>$, for use in characterizing the effect of the proteins.

During heating, the plots of c_0^{out} at different values of X_{PC} (Fig. 4) shifted vertically. The y intercept changed linearly with temperature (T) (Fig. 5). The slopes were temperature invariant (Fig. 5). As reported previously (32), heating produced the same linear change in the intrinsic curvature for each phospholipid, such that the difference between them remained constant. In the absence of the proteins, the relationship $c_0^{out} = aT + b + \Delta X_{PC}$, for constants a and b, adequately described the variation of c^{out} with both temperature and lipid composition.

Effect of the proteins

For samples that also contained the proteins, the effect of the lipids remained generally unchanged. With any particular content of the proteins, increasing X_{PC} still produced a linear decrease in c^{out} (Fig. 6). The noise in the measurements increased with larger amounts of the proteins, which are notoriously difficult to work with because of their extreme hydrophobicity. The data nonetheless continued to fit, at least roughly, a linear dependence on X_{PC}. These plots with different amounts of proteins also shared a common y intercept at $X_{PC} = 0$ (Fig. 6), such that $c^{out} = c_{PE}^{out} + \alpha X_{PC}$. The common y intercept agreed with our prior finding that the proteins had no effect on c^{out} for DOPE alone (22).

The added proteins changed the magnitude of the response to X_{PC}. With larger amounts of protein, adding DOPC produced a smaller reduction in c^{out} (Fig. 6). The slope, α, of these linear plots was independent of temperature and determined only by *SP* (Fig. 7), starting from a common value for the lipids alone, such that $\alpha = \alpha_0 + \alpha_1 SP$, and

$$\begin{aligned} c^{out} &= c_{PE}^{out} + (\alpha_0 + \alpha_1 SP) X_{PC} \\ &= c_0^{out} + \alpha_1 SP X_{PC} \end{aligned}.$$

The proteins produced an initially linear decrease in the magnitude of α (Fig. 7). This effect saturated at high *SP*,

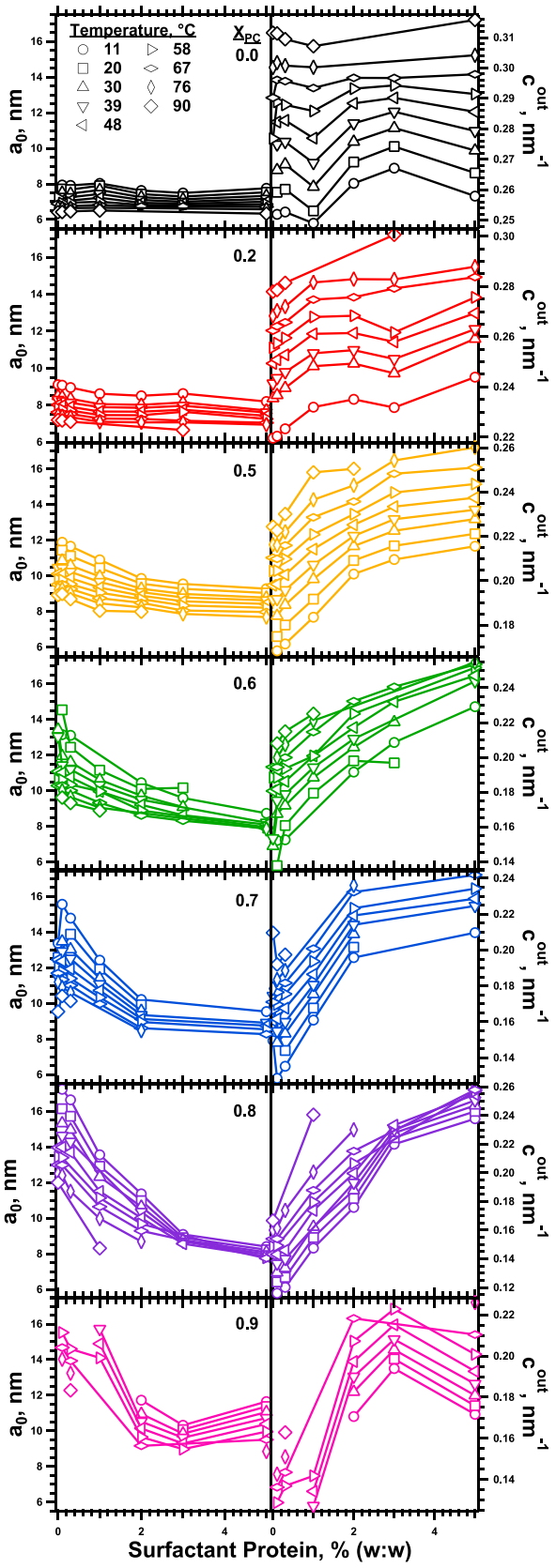

FIGURE 3 Response of the cylindrical phospholipid monolayers to the surfactant proteins. The panels share a common x axis. In the left column, which presents the lattice constant (a_0) (*left axis*) for the H_{II} phase, the range of the y axis is common to all panels, emphasizing the variation among samples with different X_{PC}. In the right column, which gives c^{out} (*right axis*), the different scales in the panels emphasize the shape of the curves. The samples, which contain 16% (w/w) tetradecane in addition to the phospholipids and proteins, were dispersed in buffered electrolyte (HSC). To see this figure in color, go online.

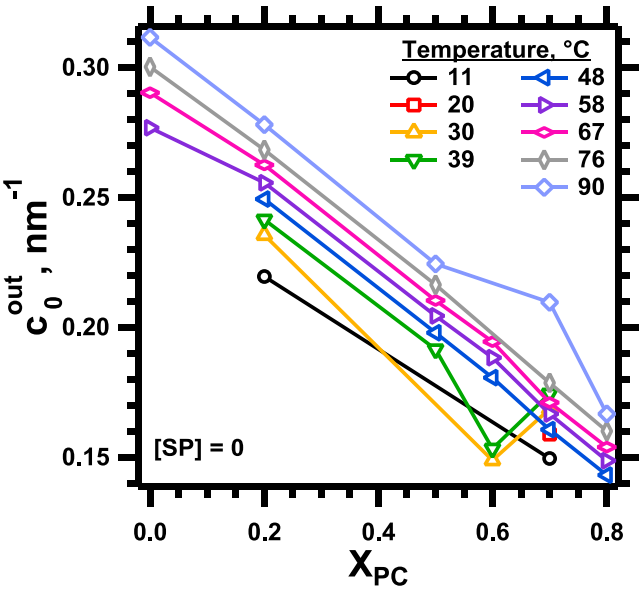

FIGURE 4 Effect of lipid composition on c_0^{out} for samples without proteins. To see this figure in color, go online.

where the slopes approached a value of minimum magnitude (Fig. 7).

The Langmuir model of binding to a finite number of sites on a surface (43) provided one example of behavior that would saturate. The fraction of occupied sites, θ, would approach a maximum. For a concentration of bound protein, SP_b, given by $SP_b = \theta\, SP_b^m$, where SP_b^m is the maximum capacity of bound protein, the Langmuir equation indicates that $\theta = K_a\, SP_f/(1 + K_a\, SP_f)$, for an association constant, K_a, and a concentration of free protein, SP_f. The low concentrations of protein used here allowed expression of θ in terms of SP, the total added protein, rather than SP_f according to $\theta = \epsilon\, SP/(1 + \epsilon\, SP)$, where $\epsilon = K_a/(1 + K_a\, SP_b^m)$ (Supporting Materials and Methods). For protein with an intrinsic curvature of c_{sp}^{out}, the change induced by the proteins, $\Delta c^{out} \equiv c^{out} - c_0^{out}$, would be given by

$$\begin{aligned}\Delta c^{out} &= \alpha_1\, SP\, X_{PC} \\ &= c_{sp}^{out}\, \theta\, \frac{SP_b^m}{PL} = c_{sp}^{out}\, \frac{\epsilon\, SP}{1 + \epsilon\, SP}\, \frac{SP_b^m}{PL}, \\ &= \frac{a_1\, SP}{1 + a_2\, SP}\, X_{PC}\end{aligned}$$

where $a_1\, X_{PC} = c_{sp}^{out}\, \epsilon\, SP_b^m/PL$, $a_2 = \epsilon$, and PL is the phospholipid concentration.

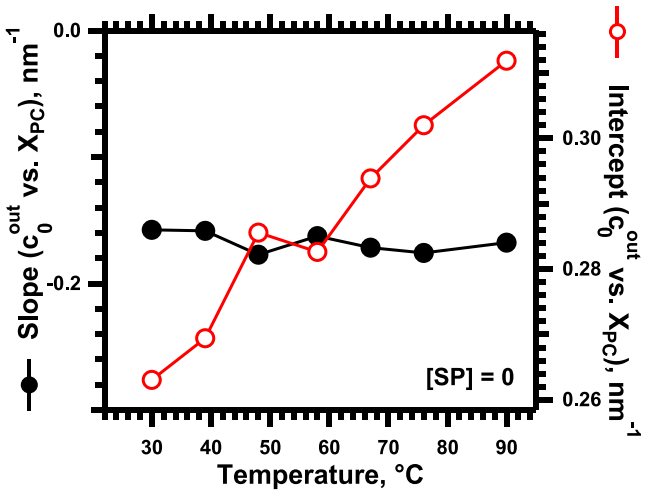

FIGURE 5 Effect of temperature on the response of c_0^{out} to changes in composition for the lipids without proteins. The graph gives the slope (*solid symbols*, *left axis*) and intercept at $X_{PC} = 0$ (*open symbols*, *right axis*) of the best linear fits to the data in Fig. 4. To see this figure in color, go online.

This expression, based on how X_{PC} affected c^{out}, reasonably fit the response of c^{out} to added protein, and how temperature and X_{PC} altered that response (Fig. 8). The composite equation described the data well over the range of lipid compositions from $X_{PC} = 0$–0.8 and temperatures of 11–76°C. For the range of 0–3%, *SP* produced a roughly linear increase in c^{out}, which then approached a maximum (Fig. 8). As predicted by the equation, the initial slope was roughly proportional to X_{PC} (Fig. 9 *A*) but independent of temperature (Fig. 9 *B*).

The composite equation allowed extrapolation to systems that were experimentally inaccessible because they failed to form H_{II} structures, such as proteins with pure DOPC, where the effect should be greatest. For large SP,Δc^{out} would reach a maximum value of $(a_1/a_2)X_{pc}$. At $X_{PC} = 1$ and 39°C, using values averaged over the range of $X_{PC} = 0.5$–0.8 for a_1 and a_2 of 0.035 nm^{-1} × (% protein)$^{-1}$ and 0.29 (% protein)$^{-1}$, respectively (Fig. 10), the proteins would produce a maximum change in c^{out} of 0.12 nm^{-1}.

DISCUSSION

Proteins induce negative curvature

Our results show that hydrophobic surfactant proteins, when combined with the appropriate phospholipids, increase curvature (Fig. 3). This effect depends on the composition of the lipids. As shown previously (22), with lipids that contain only DOPE, the proteins produce no effect. With progressively larger amounts of DOPC, the proteins induce a dose-related increase in c^{out} (Fig. 8). The effect is not subtle, with changes produced by the proteins reaching 100%.

The change in c^{out} almost certainly corresponds to a shift in the spontaneous curvature. In a bent sheet with finite thickness, curvature depends on the choice of the layer at which the radius is measured. The H_{II} lattice constant provides the radius at the outer surface of the phospholipid monolayer (Fig. 1 *A*). Spontaneous curvature is defined instead at the neutral plane, where the energies of bending and area-compression uncouple, and approximated at the more experimentally accessible pivotal plane, where the cross-sectional molecular area remains constant during bending (4). Generally, the pivotal plane is located at the level of the glycerol group in the phospholipid (Fig. 1 *A*) (44). Although it is unusual, factors can shift the pivotal plane to a different location along the phospholipid (45). Theoretically, the pivotal plane could remain at the same radius despite a change in the outer diameter. The proteins could therefore alter c^{out} without affecting spontaneous curvature. That possibility seems most unlikely. The changes in the outer radius demonstrated here approach 9 nm, well beyond the thickness of a monolayer. Our previous studies with DOPE:DOPG demonstrated that the outer surface was separated from the pivotal plane by ~1.1 nm (22). Using that difference here to estimate the location of the pivotal plane, we found that the proteins would change spontaneous curvature by as much as 113%.

Our results support the model in which proteins promote adsorption by changing curvature. Several observations suggested that adsorption proceeds via a negatively curved, rate-limiting intermediate that connects the adsorbing vesicle to the interfacial film. Previously, however, direct evidence that proteins can produce the structural changes that would promote formation of the intermediate was limited (22). Our demonstration of the proteins' ability to produce a large shift in curvature toward the configuration of the hypothetical intermediate provides that evidence.

Our studies leave untested an alternative mechanism by which proteins could reduce the energy of bending. For any given spontaneous curvature, more flexible leaflets would bend more easily to a configuration with different curvature (4). Our experiments provide no information on whether proteins affect the modulus of either simple-splay or saddle-splay bending, and if so, how the consequences of such changes would compare with their effects on curvature. Our results do provide direct evidence that hydrophobic surfactant proteins produce a large increase in negative curvature. According to the model of adsorption via a tightly curved intermediate, these structural alterations by the proteins may well be sufficient to explain their function.

Our results enhance the evidence that fusogenic proteins can induce negative curvature. Several examples of proteins that induce positive curvature have been reported (1,46), but evidence for proteins that induce negative curvature has been largely indirect. The structures formed by lipids with spontaneous curvature are determined by the balance between the energies of bending and chain packing (47,48). Several peptides with amphipathic helices, including both the combined surfactant proteins (37) and isolated SP-B (36), convert lamellar lipids to Q_{II} phases (49,50). Other

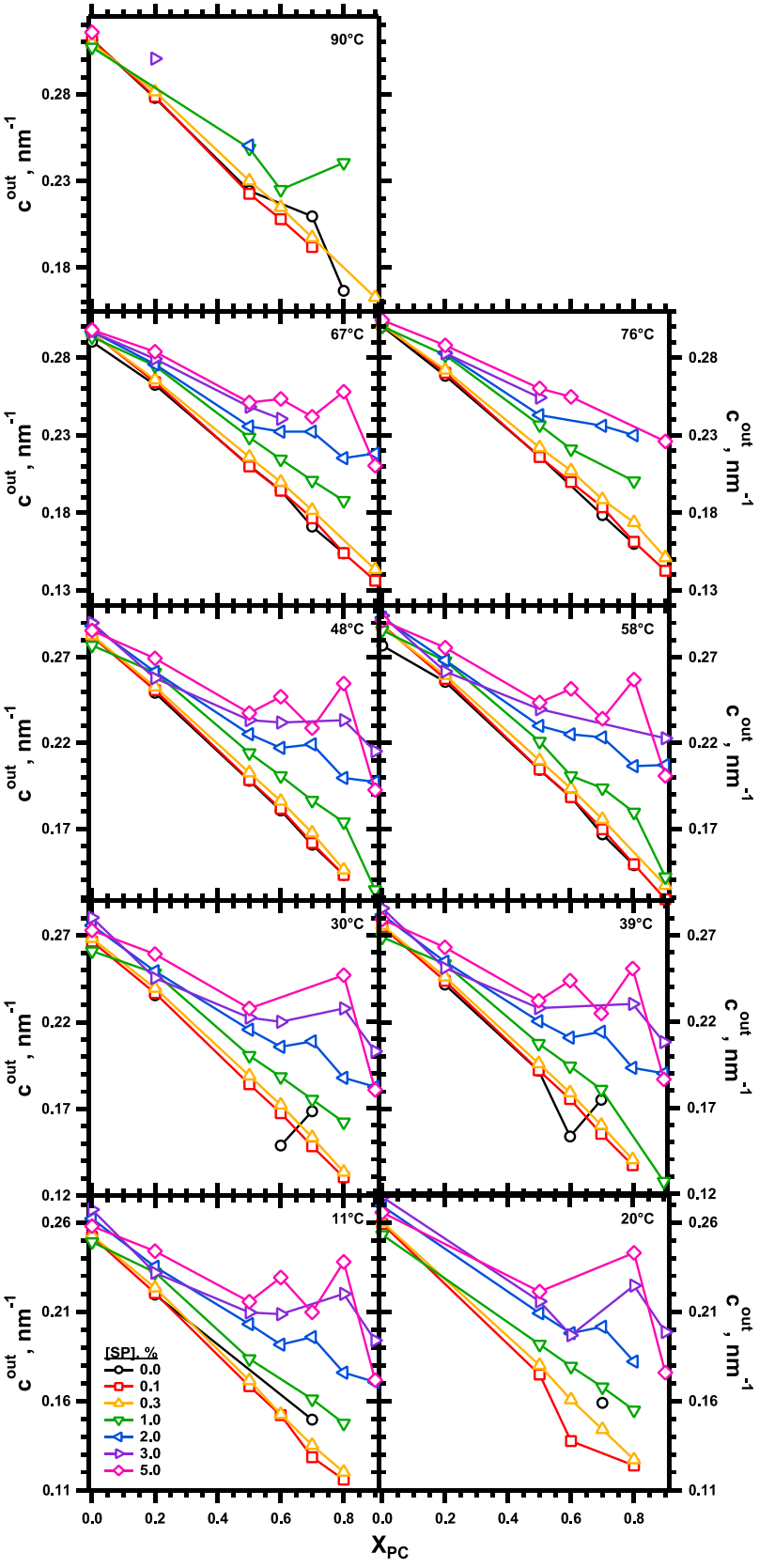

FIGURE 6 Variation of c^{out} with X_{PC} for the full set of samples. Each panel gives results for a specific temperature, with each curve representing the data for a specific concentration of protein. To see this figure in color, go online.

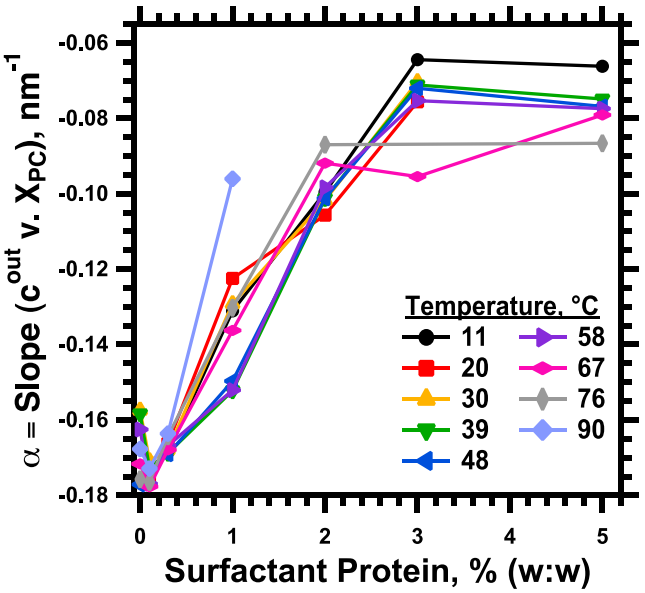

FIGURE 7 Effect of the proteins on the response of c^{out} to changes in X_{PC}. The slopes from linear fits to the variation of c^{out} with X_{PC} (Fig. 6) are plotted against the different concentrations of protein at each temperature. To see this figure in color, go online.

peptides with similar helical elements lower the temperature of the lamellar-to-H_{II} transition (6,11,49,51,52). The peptides could achieve the structural changes in both the Q_{II} and H_{II} phases by inducing a more negative spontaneous curvature. The transitions to both inverse phases, however, involve chain packing as well as curvature. Neither the dimensions of the Q_{II} phase nor shifts in transition temperatures measure the curvature of a leaflet. The results presented here directly confirm that surfactant proteins induce a more negative curvature and provide quantitative information about the extent of those effects.

Our findings suggest the location occupied by the proteins within the lipid leaflet. To change a leaflet such that its hydrophilic face becomes more concave, the proteins would preferentially expand the hydrophobic side of the monolayer. The changes demonstrated here presumably reflect mainly the influence of the proteins on the phospholipid acyl chains. SP-C, with a hydrophobic sequence appropriate to span a bilayer (53), has much less ability than SP-B to affect adsorption (54) or induce formation of Q_{II} phases (36). Our results imply that SP-B inserts deep within the hydrophobic portions of the phospholipid leaflet.

The changes that occur during heating fit with the classical view that the curvature of a monolayer reflects the effective shape of its constituents (55–57). As reported previously (32), higher temperature increases the intrinsic curvature for each phospholipid, consistent with the thermal expansion of the acyl chains and the hydrophobic cross-sectional area. An equal expansion of the hydrophobic area for the two compounds would explain why the difference between the two intrinsic curvatures at different temperatures remains fixed (32). Heating also has no effect on the response of curvature to the added proteins, suggesting that their effective shape is constant. Both SP-B and SP-C contain a high content of α-helix (58), the dimensions of which should remain unchanged during heating. The temperature-invariant effect of the proteins is at least consistent with alterations in curvature induced by their helical segments.

Our results fit with our prior findings. The conversion by the proteins of lamellar 1-palmitoyl-2-oleoyl phosphatidylethanolamine to cubic phases (36,37) suggests an effect on curvature. The changes in the DOPE:DOPG cylinders (22) were relatively small, but they demonstrated a dose-related effect of the proteins on curvature. Stabilizing the large cylindrical monolayers here required the addition of tetradecane. The alkane could alter the effects of the proteins. Together with our prior studies, which included no alkane, our results seem most likely to reflect only the interaction of the proteins with the phospholipids.

Dependence on lipid composition

The composition of the lipids alters the response of curvature to the proteins. The mechanism of this compositional dependence is less important than whether the effect of the proteins extends from these model lipids to the biological mixture. Phosphatidylcholines dominate the composition of pulmonary surfactant, constituting ~82% (mol/mol) of the phospholipids, well above the ~3% of phosphatidylethanolamine (27). The spontaneous curvature of leaflets formed by the surfactant lipids should be low. The ability of the proteins to change curvature, as demonstrated here using leaflets with low spontaneous curvature and high levels of DOPC, should extend to the physiological system.

The mechanism by which the lipids alter the effect of the proteins is somewhat obscure. The change induced by the proteins should be given by $\Delta c^{out} \approx c_{sp}^{out}\, SP_b/PL$ for the low amounts of protein used here (Supporting Materials and Methods). The extreme hydrophobicity of the surfactant proteins, however, complicates any effort to establish the amount of bound protein. Any protein that is not inserted into the cylindrical monolayer is much more likely to associate with another hydrophobic surface, such as the exterior of the H_{II} phase, than to remain free in the aqueous medium. Approaches commonly used to distinguish bound from free protein may well be inadequate here. This problem limits our ability to reach hard conclusions concerning the mechanisms by which the lipids alter the effect of the proteins on curvature.

In samples that contain the proteins, the response of curvature to any of the variables could in theory reflect changes in c_{sp}^{out}, SP_b, or both. A change in the intrinsic curvature of the proteins, however, seems unlikely. Prior studies with other constituents produced additive effects on curvature in which the molecular contribution remained constant (48). The temperature invariance of the response to added protein supports a fixed molecular shape here. We assume

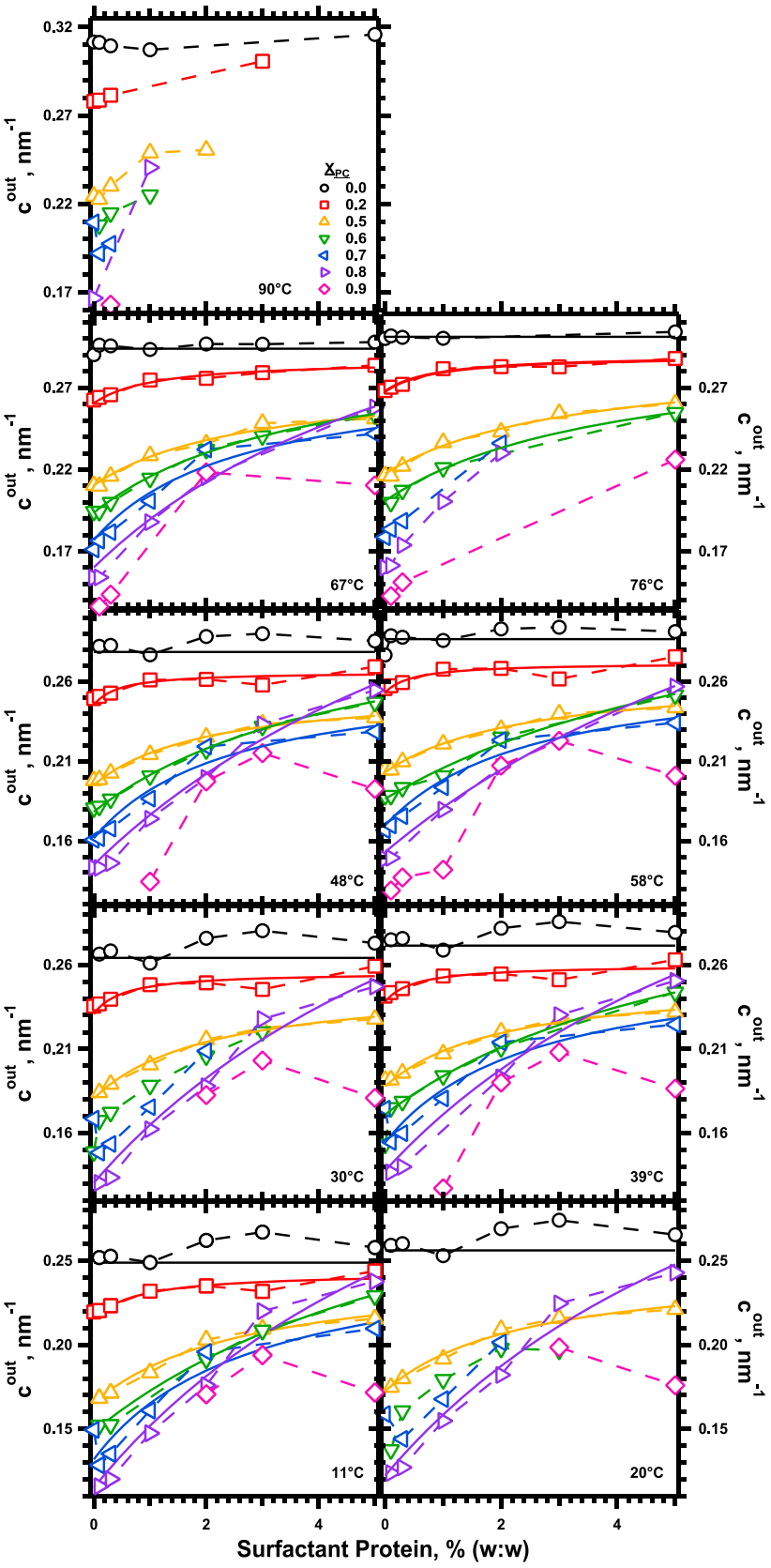

FIGURE 8 Dependence of c^{out} on the concentration of protein. Each panel gives the data for a specific temperature, with each trace providing results for a specific X_{PC}. The continuous curves give the best fit of the equation $c^{out} = \langle c_0^{out} \rangle + a_1 SP/(1 + a_2 SP X_{PC})$ to data (connected by *dashed lines*) that included measurements over the full range of protein concentrations. a_1 and a_2 are fitting parameters. $\langle c_0^{out} \rangle$ is the average value of c_0^{out} for a particular set of lipids, calculated from the linear fit for that temperature in Fig. 4. To see this figure in color, go online.

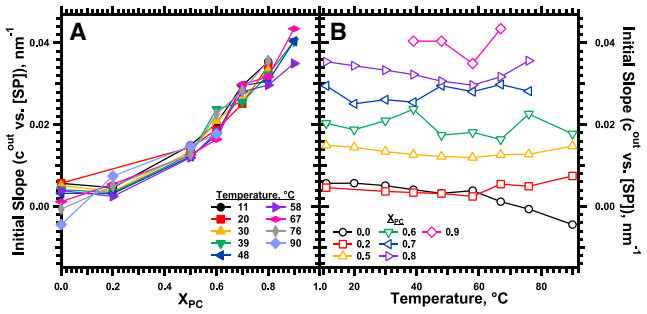

FIGURE 9 Initial response of c^{out} to SP. Linear fits of c^{out} to SP (Fig. 8) for the range of 0–3% protein provided the initial slopes. (*A*) Dependence on X_{PC} at constant temperatures. (*B*) Effect of temperature for samples with fixed X_{PC}. To see this figure in color, go online.

that the variation of curvature in response to added protein, and the alteration of that response with different lipids, both reflect changes in SP_b.

Binding to bilayers is commonly considered in terms of partitioning between the membrane and the surrounding aqueous environment (31,59–62). For our studies with the H_{II} phase, this approach has problems. With a partition coefficient that remains constant, binding would not saturate until X_{sp} approaches 1, well above the amounts of protein used here. A partition coefficient that varies suitably could, of course, cause saturation. Alamethicin provides an example of a peptide for which the partition coefficient varies with the spontaneous curvature of the leaflets in a bilayer. Presumably an appropriate variation of the partition coefficient for the H_{II} phase and the surrounding water could explain the behavior of our data.

The Langmuir model of binding to a limited number of sites on a surface (43) instead explains saturation directly. The bound protein, given by $\theta\, SP_b^m$, will saturate when θ approaches its maximum value. Concerning the effect of the lipids, our results suggest that their composition at least changes SP_b^m. The model predicts that $(a_1/a_2)\, X_{PC}$ is proportional to $c_{sp}^{out}\, SP_b^m$ (Supporting Materials and Methods). Our results show that $(a_1/a_2)\, X_{PC}$ increases with greater X_{PC} (Fig. 10 *C*). If c_{sp}^{out} is constant, then SP_b^m must increase at higher X_{PC}. The larger cylinders with lower curvature produced with larger amounts of DOPC would accommodate greater amounts of protein.

The radius of the cylindrical monolayers provides an obvious mechanism by which the lipids might alter the binding capacity. Cylinders of any radius should exclude proteins above a certain size. Contact between proteins at adjacent sites might also limit binding to a curved surface below the capacity of a planar monolayer. The limited information available regarding the structure of the proteins complicates assessment of these possibilities. The primary sequence of SP-B (63), which is the larger of the two proteins, along with its secondary structure as assessed by vibrational spectroscopy (53) and the disulfide cross-links within the monomers all suggest that the chain forms pairs

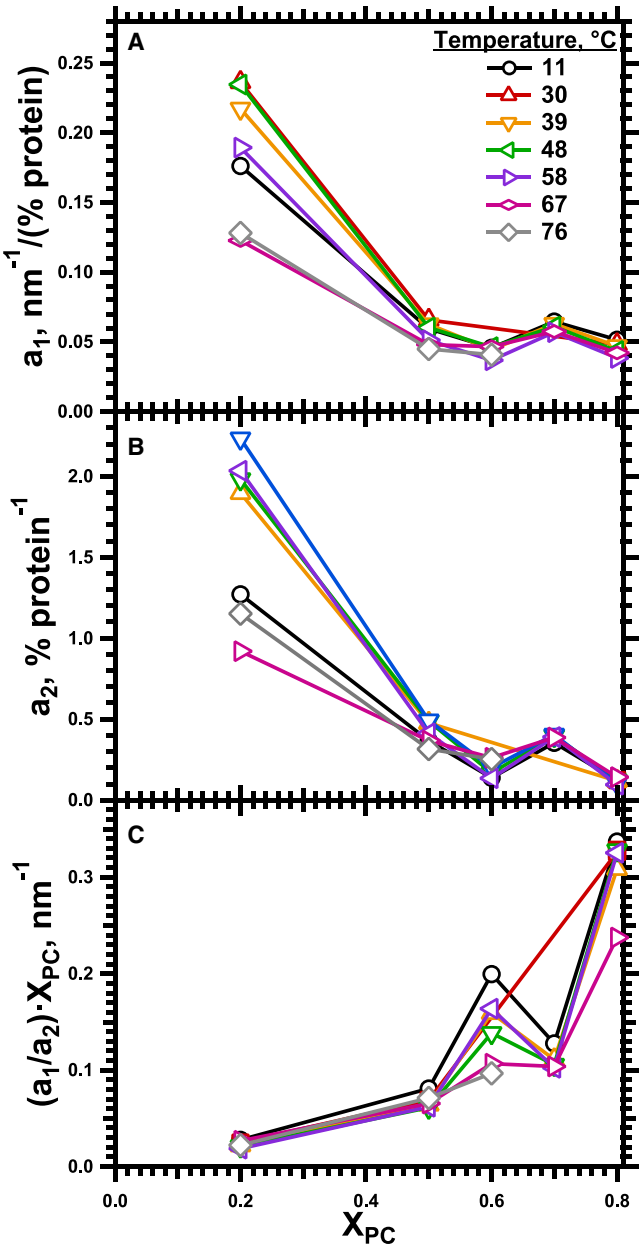

FIGURE 10 Dependence on X_{PC} of the parameters that describe the variation of c^{out}. Fits of the data to $c^{out} = \langle c_0^{out} \rangle + a_1\, SP/(1 + a_2\, SP\, X_{PC})$ (Fig. 8) provided the basis for calculating (*A*), a_1; (*B*), a_2; (*C*), $(a_1/a_2)\, X_{PC}$. To see this figure in color, go online.

of antiparallel helices. The cross-link between monomers suggests that the pairs from the two chains might be parallel, and that a quartet of helices might determine the smallest cross-sectional dimension. For a helical diameter of 1.1 nm (64), that smallest dimension would be ~3.1 nm. The aqueous core should be larger. The proteins cease to affect curvature when the outer radius reaches ~8 nm (Fig. 3). For monolayers with the same thickness as DOPE:-DOPG of ~1.3 nm (22), the aqueous core would have a diameter of ~5.4 nm. Particularly in light of the uncertainties, the consequences of the relative sizes for the

cylindrical monolayer and the proteins are unclear. The general observation remains that when the external diameter is reduced to a certain value, whether by increasing protein or DOPE, the proteins cease to affect curvature. Restriction of the binding capacity by the cylindrical size provides a reasonable but unproven explanation.

Our analysis based on the Langmuir model is tenuous. Our experiments tested only the ability of the model to describe the data. We consider the model useful primarily for clarifying the different mechanisms by which the lipids could produce their effect. Our primary result, however, is not that the lipids alter the effect of the proteins, but that, given the correct conditions, the proteins produce a large change in curvature.

CONCLUSION

The relatively few reported studies that have measured how other fusogenic proteins affect spontaneous curvature used H_{II} structures with approximately the diameter for DOPE (7,9,10,12,65,66). Surfactant proteins, which double the curvature for larger cylinders, produce no change with DOPE. Whether other fusogenic proteins would produce larger changes with a greater cylindrical diameter, or whether the effect of the surfactant proteins is exceptional, remains unknown.

SUPPORTING MATERIAL

Supporting Information is available at http://www.biophysj.org/biophysj/supplemental/S0006-3495(15)00542-1.

AUTHOR CONTRIBUTIONS

M.C. designed the experiments, conducted the research, and analyzed and interpreted the results. R.W.L. conducted the research and analyzed the data. S.B.R. interpreted results and participated in writing the manuscript. S.B.H. conceived and designed the studies, and wrote the manuscript.

ACKNOWLEDGMENTS

Dr. Edmund Egan of ONY, Inc. provided the extracted calf surfactant from which the surfactant proteins were obtained. Leonard E. Schulwitz Jr. and Hamed Khoojinian contributed computer programs that greatly accelerated the analysis of the diffraction patterns.

This work was supported by the National Institutes of Health (NIH, grant HL54209). Measurements were performed at the SLAC National Accelerator Laboratory, Stanford Synchrotron Radiation Lightsource (SSRL), which is supported by the Office of Basic Energy Sciences, Office of Science, U.S. Department of Energy (DOE), under contract No. DE-AC02-76SF00515. The SSRL Structural Molecular Biology Program is supported by the DOE Office of Biological and Environmental Research and by the National Institute of General Medical Sciences (NIGMS), NIH, including grant P41GM103393. The contents of this publication are solely the responsibility of the authors and do not necessarily represent the official views of the NIGMS or NIH.

REFERENCES

1. Zimmerberg, J., and M. M. Kozlov. 2006. How proteins produce cellular membrane curvature. *Nat. Rev. Mol. Cell Biol.* 7:9–19.
2. Markin, V. S., M. M. Kozlov, and V. L. Borovjagin. 1984. On the theory of membrane fusion. The stalk mechanism. *Gen. Physiol. Biophys.* 3:361–377.
3. Chernomordik, L., A. Chanturiya, …, J. Zimmerberg. 1995. The hemifusion intermediate and its conversion to complete fusion: regulation by membrane composition. *Biophys. J.* 69:922–929.
4. Helfrich, W. 1973. Elastic properties of lipid bilayers: theory and possible experiments. *Z. Naturforsch. C.* 28:693–703.
5. Tamm, L. K., and X. Han. 2000. Viral fusion peptides: a tool set to disrupt and connect biological membranes. *Biosci. Rep.* 20:501–518.
6. Koller, D., and K. Lohner. 2014. The role of spontaneous lipid curvature in the interaction of interfacially active peptides with membranes. *Biochim. Biophys. Acta.* 1838:2250–2259.
7. Colotto, A., I. Martin, …, R. M. Epand. 1996. Structural study of the interaction between the SIV fusion peptide and model membranes. *Biochemistry.* 35:980–989.
8. Davies, S. M., R. F. Epand, …, R. M. Epand. 1998. Modulation of lipid polymorphism by the feline leukemia virus fusion peptide: implications for the fusion mechanism. *Biochemistry.* 37:5720–5729.
9. Siegel, D. P., and R. M. Epand. 2000. Effect of influenza hemagglutinin fusion peptide on lamellar/inverted phase transitions in dipalmitoleoylphosphatidylethanolamine: implications for membrane fusion mechanisms. *Biochim. Biophys. Acta.* 1468:87–98.
10. Epand, R. M., and R. F. Epand. 2000. Modulation of membrane curvature by peptides. *Biopolymers.* 55:358–363.
11. Epand, R. M. 2003. Fusion peptides and the mechanism of viral fusion. *Biochim. Biophys. Acta.* 1614:116–121.
12. Tristram-Nagle, S., R. Chan, …, J. F. Nagle. 2010. HIV fusion peptide penetrates, disorders, and softens T-cell membrane mimics. *J. Mol. Biol.* 402:139–153.
13. Poulain, F. R., S. Nir, and S. Hawgood. 1996. Kinetics of phospholipid membrane fusion induced by surfactant apoproteins A and B. *Biochim. Biophys. Acta.* 1278:169–175.
14. Ryan, M. A., X. Qi, …, T. E. Weaver. 2005. Mapping and analysis of the lytic and fusogenic domains of surfactant protein B. *Biochemistry.* 44:861–872.
15. Rugonyi, S., S. C. Biswas, and S. B. Hall. 2008. The biophysical function of pulmonary surfactant. *Respir. Physiol. Neurobiol.* 163: 244–255.
16. Sen, A., S.-W. Hui, …, E. A. Egan. 1988. Localization of lipid exchange sites between bulk lung surfactants and surface monolayer: freeze fracture study. *J. Colloid Interface Sci.* 126:355–360.
17. Schürch, S., D. Schürch, …, B. Robertson. 1994. Surface activity of lipid extract surfactant in relation to film area compression and collapse. *J. Appl. Physiol.* 77:974–986.
18. Haller, T., P. Dietl, …, G. Putz. 2004. Tracing surfactant transformation from cellular release to insertion into an air-liquid interface. *Am. J. Physiol. Lung Cell. Mol. Physiol.* 286:L1009–L1015.
19. Yu, S.-H., P. G. R. Harding, and F. Possmayer. 1984. Artificial pulmonary surfactant. Potential role for hexagonal H_{II} phase in the formation of a surface-active monolayer. *Biochim. Biophys. Acta.* 776:37–47.
20. Perkins, W. R., R. B. Dause, …, A. S. Janoff. 1996. Role of lipid polymorphism in pulmonary surfactant. *Science.* 273:330–332.
21. Biswas, S. C., S. B. Rananavare, and S. B. Hall. 2005. Effects of gramicidin-A on the adsorption of phospholipids to the air-water interface. *Biochim. Biophys. Acta.* 1717:41–49.
22. Chavarha, M., R. W. Loney, …, S. B. Hall. 2013. An anionic phospholipid enables the hydrophobic surfactant proteins to alter spontaneous curvature. *Biophys. J.* 104:594–603.

23. Biswas, S. C., S. B. Rananavare, and S. B. Hall. 2007. Differential effects of lysophosphatidylcholine on the adsorption of phospholipids to an air/water interface. *Biophys. J.* 92:493–501.
24. Walters, R. W., R. R. Jenq, and S. B. Hall. 2000. Distinct steps in the adsorption of pulmonary surfactant to an air-liquid interface. *Biophys. J.* 78:257–266.
25. Schram, V., and S. B. Hall. 2001. Thermodynamic effects of the hydrophobic surfactant proteins on the early adsorption of pulmonary surfactant. *Biophys. J.* 81:1536–1546.
26. Klenz, U., M. Saleem, …, H. J. Galla. 2008. Influence of lipid saturation grade and headgroup charge: a refined lung surfactant adsorption model. *Biophys. J.* 95:699–709.
27. Kahn, M. C., G. J. Anderson, …, S. B. Hall. 1995. Phosphatidylcholine molecular species of calf lung surfactant. *Am. J. Physiol.* 269:L567–L573.
28. Johansson, J., T. Curstedt, and H. Jörnvall. 1991. Surfactant protein B: disulfide bridges, structural properties, and kringle similarities. *Biochemistry.* 30:6917–6921.
29. Haagsman, H. P., and R. V. Diemel. 2001. Surfactant-associated proteins: functions and structural variation. *Comp. Biochem. Physiol. A Mol. Integr. Physiol.* 129:91–108.
30. Alley, S. H., O. Ces, …, R. H. Templer. 2008. X-ray diffraction measurement of the monolayer spontaneous curvature of dioleoylphosphatidylglycerol. *Chem. Phys. Lipids.* 154:64–67.
31. Lewis, J. R., and D. S. Cafiso. 1999. Correlation between the free energy of a channel-forming voltage-gated peptide and the spontaneous curvature of bilayer lipids. *Biochemistry.* 38:5932–5938.
32. Tate, M. W., and S. M. Gruner. 1989. Temperature dependence of the structural dimensions of the inverted hexagonal (H_{II}) phase of phosphatidylethanolamine-containing membranes. *Biochemistry.* 28:4245–4253.
33. Takahashi, A., and T. Fujiwara. 1986. Proteolipid in bovine lung surfactant: its role in surfactant function. *Biochem. Biophys. Res. Commun.* 135:527–532.
34. Hawgood, S., B. J. Benson, …, R. T. White. 1987. Nucleotide and amino acid sequences of pulmonary surfactant protein SP 18 and evidence for cooperation between SP 18 and SP 28-36 in surfactant lipid adsorption. *Proc. Natl. Acad. Sci. USA.* 84:66–70.
35. Hall, S. B., Z. Wang, and R. H. Notter. 1994. Separation of subfractions of the hydrophobic components of calf lung surfactant. *J. Lipid Res.* 35:1386–1394.
36. Chavarha, M., R. W. Loney, …, S. B. Hall. 2012. Differential effects of the hydrophobic surfactant proteins on the formation of inverse bicontinuous cubic phases. *Langmuir.* 28:16596–16604.
37. Chavarha, M., H. Khoojinian, …, S. B. Hall. 2010. Hydrophobic surfactant proteins induce a phosphatidylethanolamine to form cubic phases. *Biophys. J.* 98:1549–1557.
38. van Eijk, M., C. G. De Haas, and H. P. Haagsman. 1995. Quantitative analysis of pulmonary surfactant proteins B and C. *Anal. Biochem.* 232:231–237.
39. Liu, S., L. Zhao, …, G. A. Lajoie. 2008. Characterization of bovine surfactant proteins B and C by electrospray ionization mass spectrometry. *Rapid Commun. Mass Spectrom.* 22:197–203.
40. Sun, R. G., and J. Zhang. 2004. The cubic phase of phosphatidylethanolamine film by small angle x-ray scattering. *J. Phys. D Appl. Phys.* 37:463–467.
41. Rand, R. P., N. L. Fuller, …, V. A. Parsegian. 1990. Membrane curvature, lipid segregation, and structural transitions for phospholipids under dual-solvent stress. *Biochemistry.* 29:76–87.
42. Hyde, S. 1997. The Language of Shape: The Role of Curvature in Condensed Matter—Physics, Chemistry, and Biology. Elsevier, New York/Amsterdam.
43. Langmuir, I. 1916. The constitution and fundamental properties of solids and liquids. Part I. Solids. *J. Am. Chem. Soc.* 38:2221–2295.
44. Kozlov, M. M. 2007. Determination of lipid spontaneous curvature from X-ray examinations of inverted hexagonal phases. *Methods Mol. Biol.* 400:355–366.
45. Chen, Z., and R. P. Rand. 1998. Comparative study of the effects of several n-alkanes on phospholipid hexagonal phases. *Biophys. J.* 74:944–952.
46. Baumgart, T., B. R. Capraro, …, S. L. Das. 2011. Thermodynamics and mechanics of membrane curvature generation and sensing by proteins and lipids. *Annu. Rev. Phys. Chem.* 62:483–506.
47. Charvolin, J., and J. F. Sadoc. 1987. Periodic systems of frustrated fluid films and "bicontinuous" cubic structures in liquid crystals. *J. Phys. (Paris).* 48:1559–1569.
48. Gruner, S. M. 1989. Stability of lyotropic phases with curved interfaces. *J. Phys. Chem.* 93:7562–7570.
49. Siegel, D. P. 2005. The relationship between bicontinuous inverted cubic phases and membrane fusion. *In* Bicontinuous Liquid Crystals. M. L. Lynch and P. T. Spicer, editors. Taylor & Francis, Boca Raton, pp. 59–98.
50. Schmidt, N. W., and G. C. L. Wong. 2013. Antimicrobial peptides and induced membrane curvature: geometry, coordination chemistry, and molecular engineering. *Curr. Opin. Solid State Mater. Sci.* 17:151–163.
51. Haney, E. F., S. Nathoo, …, E. J. Prenner. 2010. Induction of nonlamellar lipid phases by antimicrobial peptides: a potential link to mode of action. *Chem. Phys. Lipids.* 163:82–93.
52. Epand, R. M. 1998. Lipid polymorphism and protein-lipid interactions. *Biochim. Biophys. Acta.* 1376:353–368.
53. Vandenbussche, G., A. Clercx, …, J. M. Ruysschaert. 1992. Secondary structure and orientation of the surfactant protein SP-B in a lipid environment. A Fourier transform infrared spectroscopy study. *Biochemistry.* 31:9169–9176.
54. Wang, Z., O. Gurel, …, R. H. Notter. 1996. Differential activity and lack of synergy of lung surfactant proteins SP-B and SP-C in interactions with phospholipids. *J. Lipid Res.* 37:1749–1760.
55. Tartar, H. V. 1955. A theory of the structure of the micelles of normal paraffin-chain salts in aqueous solution. *J. Phys. Chem.* 59:1195–1199.
56. Tanford, C. 1973. The Hydrophobic Effect: Formation of Micelles and Biological Membranes. Wiley, New York.
57. Israelachvili, J. N., D. J. Mitchell, and B. W. Ninham. 1976. Theory of self-assembly of hydrocarbon amphiphiles into micelles and bilayers. *J. Chem. Soc., Faraday Trans. 2.* 72:1525–1568.
58. Johansson, J., T. Curstedt, and B. Robertson. 1994. The proteins of the surfactant system. *Eur. Respir. J.* 7:372–391.
59. Ketterer, B., B. Neumcke, and P. Läuger. 1971. Transport mechanism of hydrophobic ions through lipid bilayer membranes. *J. Membr. Biol.* 5:225–245.
60. Cafiso, D. S., and W. L. Hubbell. 1981. EPR determination of membrane potentials. *Annu. Rev. Biophys. Bioeng.* 10:217–244.
61. Flewelling, R. F., and W. L. Hubbell. 1986. Hydrophobic ion interactions with membranes. Thermodynamic analysis of tetraphenylphosphonium binding to vesicles. *Biophys. J.* 49:531–540.
62. Shintou, K., M. Nakano, …, T. Handa. 2007. Interaction of an amphipathic peptide with phosphatidycholine/phosphatidylethanolamine mixed membranes. *Biophys. J.* 93:3900–3906.
63. Curstedt, T., J. Johansson, …, H. Jörnvall. 1988. Low-molecular-mass surfactant protein type 1. The primary structure of a hydrophobic 8-kDa polypeptide with eight half-cystine residues. *Eur. J. Biochem.* 172:521–525.
64. Hristova, K., W. C. Wimley, …, S. H. White. 1999. An amphipathic alpha-helix at a membrane interface: a structural study using a novel X-ray diffraction method. *J. Mol. Biol.* 290:99–117.
65. Szule, J. A., and R. P. Rand. 2003. The effects of gramicidin on the structure of phospholipid assemblies. *Biophys. J.* 85:1702–1712.
66. Harroun, T. A., K. Balali-Mood, …, J. P. Bradshaw. 2003. The fusion peptide of simian immunodeficiency virus and the phase behaviour of N-methylated dioleoylphosphatidylethanolamine. *Biochim. Biophys. Acta.* 1617:62–68.

Biophysical Journal

Supporting Material

Hydrophobic Surfactant Proteins Strongly Induce Negative Curvature

Mariya Chavarha,[1,2,3] Ryan W. Loney,[1,2,3] Shankar B. Rananavare,[4] and Stephen B. Hall[1,2,3,*]

[1]Department of Biochemistry & Molecular Biology, [2]Department of Medicine, and [3]Department of Physiology & Pharmacology, Oregon Health & Science University, Portland, Oregon; and [4]Department of Chemistry, Portland State University, Portland, Oregon

SUPPORTING INFORMATION

Additive curvature: Our analysis requires an expression for the variation of curvature, c, in response to changes in the concentration of total added protein, SP_t. Based on studies with different lipids,

$$c = \sum_i c_i \cdot X_i$$

where the c_i are the intrinsic curvatures for each component of a mixture, and X_i are their mol fractions. For the binary mixture of lipids combined with the proteins, because the tetradecane fits between the cylindrical monolayers and has no effect on curvature (48),

$$c = c_{PE} \cdot X_{PE} + c_{PC} \cdot X_{PC} + c_{sp} \cdot X_{sp}^{b}.$$

The sub- and superscripts b, f and t refer to bound, free and total moieties, respectively.

For the lipids alone,

$$c_0 \equiv c_{PE} \cdot X_{PE} + c_{PC} \cdot X_{PC}$$

For the small X_{sp} used here, the X_i for the lipids are approximately the same with and without the proteins. The change in curvature induced by the proteins, Δc, is given by

$$\Delta c \equiv c - c_0 \approx c_{sp} \cdot X_{sp}^{b}.$$

$X_{sp}^{b} = \frac{SP_b}{SP_b + PL_t}$ for concentrations of bound protein, SP_b, and total phospholipid, PL_t.

Particularly for molar concentrations, $SP_b \ll PL_t$.

$$\therefore X_{sp}^{b} \approx \frac{SP_b}{PL_t}$$

and $$\Delta c = c_{sp} \cdot \frac{SP_b}{PL_t}$$

Langmuir model: The Langmuir model of binding by the proteins to a limited concentration of discrete sites, S, provides access to SP_b. Because $SP_b = S_b$, Δc can be expressed in terms of the fraction of occupied sites, $\theta \equiv \frac{S_b}{S_t}$:

$$\Delta c = c_{sp} \cdot \frac{SP_b}{S_t} \cdot \frac{S_t}{PL_t} = c_{sp} \cdot \theta \cdot \frac{SP_b^m}{PL_t} \qquad [1]$$

where SP_b^m is the maximum possible concentration of bound protein. The association constant, K_a, is given by

$$K_a = \frac{SP_b}{SP_f \cdot S_f} = \frac{S_b}{(SP_t - S_b)\cdot(S_t - S_b)}$$

$$S_b^2 - S_b \cdot \left(S_t + SP_t + \frac{1}{K_a}\right) + SP_t \cdot S_t = 0$$

Solving the quadratic,

$$S_b = \frac{1}{2}\left(S_t + SP_t + \frac{1}{K_a}\right) \cdot \left[1 \pm \left(1 - \frac{4 \cdot SP_t \cdot S_t}{\left(S_t + SP_t + \frac{1}{K_a}\right)^2}\right)^{\frac{1}{2}}\right]$$

A series expansion for $(1-x)^{\frac{1}{2}}$ provides the square root. If the ratio, $x = \frac{4 \cdot SP_t \cdot S_t}{\left(S_t + SP_t + \frac{1}{K_a}\right)^2}$, is small, the first term of the expansion reasonably approximates the full expression. For x to be small, $\left(S_t + SP_t + \frac{1}{K_a}\right)^2 > 4 \cdot SP_t \cdot S_t$, which requires that the difference between the two terms must be positive.

$$\left(S_t + SP_t + \frac{1}{K_a}\right)^2 - 4 \cdot SP_t \cdot S_t = (S_t + SP_t)^2 + \frac{2(S_t + SP_t)}{K_a} + \frac{1}{K_a}^2 - 4 \cdot SP_t \cdot S_t$$

$$= (S_t - SP_t)^2 + \frac{2(S_t - SP_t)}{K_a} + \frac{4\,SP_t}{K_a} + \frac{1}{K_a}$$

$$= \left(S_t - SP_t + \frac{1}{K_a}\right)^2 + \frac{4\,SP_t}{K_a}$$

Because both $\left(S_t - SP_t + \frac{1}{K_a}\right)^2$ and $\frac{4\,SP_t}{K_a}$ are positive,

$$\left(S_t + SP_t + \frac{1}{K_a}\right)^2 - (4 \cdot SP_t \cdot S_t) > 0$$

$$\left(S_t + SP_t + \frac{1}{K_a}\right)^2 > (4 \cdot SP_t \cdot S_t)$$

$$\therefore x = \frac{4 \cdot SP_t \cdot S_t}{\left(S_t + SP_t + \frac{1}{K_a}\right)^2} < 1.$$

For $S_t \gg SP_t$, $x \ll 1$.

Using the expansion $(1-x)^{\frac{1}{2}} = 1 - \frac{x}{2}$,

$$S_b = \frac{1}{2} \cdot \left(S_t + SP_t + \frac{1}{K_a}\right)\left[1 \pm \left(1 - \frac{2 \cdot SP_t \cdot S_t}{\left(S_t + SP_t + \frac{1}{K_a}\right)^2}\right)\right]$$

$$= \frac{SP_t \cdot S_t}{S_t + SP_t + \frac{1}{K_a}} \qquad \text{for the root with the negative sign}$$

$$= \frac{\epsilon \cdot SP_t}{1 + \epsilon \cdot SP_t} \cdot S_t \qquad \text{for } \epsilon = \frac{K_a}{1 + K_a S_t}$$

$$\theta = \frac{S_b}{S_t} = \frac{\epsilon \cdot SP_t}{1 + \epsilon \cdot SP_t}$$

For the conditions of our experiments, where $S_t \gg SP_t$, the expression for θ has the same form as the exact expression of the Langmuir equation, $\theta = \frac{K_a \cdot SP_f}{1 + K_a \cdot SP_f}$, but in terms of the concentration of total protein, SP_t, rather than free, unbound protein, SP_f, and with ϵ replacing K_a. Note that because ϵ depends on SP_b^m as well as K_a, changes in the binding capacity as well as the binding affinity would affect how θ depends on SP_t.

From equation [1], these relationships indicate that

$$\Delta c = c_{sp} \cdot \frac{\epsilon \cdot SP_t}{1 + \epsilon \cdot SP_t} \cdot \frac{SP_b^m}{PL_t}$$

For our data, $\Delta c = \alpha_1 \cdot SP_t \cdot X_{PC}$.

$$\therefore \Delta c = \frac{a_1 \cdot SP_t}{1 + a_2 \cdot SP_t} \cdot X_{PC}$$

where $a_1 \cdot X_{PC} = c_{sp} \cdot \epsilon \cdot \frac{SP_b^m}{PL_t}$,

$a_2 = \epsilon$,

and $\frac{a_1 \cdot X_{PC}}{a_2} = c_{sp} \cdot \frac{SP_b^m}{PL_t}$